AD-A253 544

DATE	3. REPORT TYPE AND DATES COVERED
May 92	Final 15 Feb 89-14 Feb 92

4. TITLE AND SUBTITLE

Front Tracking and the Interaction of Nonlinear Waves

5. FUNDING NUMBERS

DAAL03-89-K-0017

6. AUTHOR(S)

James Glimm and John W. Grove

7. PERFORMING ORGANIZATION NAME(S) AND ADDRESS(ES)

University at Stony Brook
Stony Brook, NY 11794-3600

8. PERFORMING ORGANIZATION REPORT NUMBER

9. SPONSORING / MONITORING AGENCY NAME(S) AND ADDRESS(ES)

U. S. Army Research Office
P. O. Box 12211
Research Triangle Park, NC 27709-2211

10. SPONSORING / MONITORING AGENCY REPORT NUMBER

ARO 26616.26-MA

11. SUPPLEMENTARY NOTES

The view, opinions and/or findings contained in this report are those of the author(s) and should not be construed as an official Department of the Army position, policy, or decision, unless so designated by other documentation.

12a. DISTRIBUTION / AVAILABILITY STATEMENT

Approved for public release; distribution unlimited.

12b. DISTRIBUTION CODE

13. ABSTRACT *(Maximum 200 words)*

The research program has emphasized innovative computations and theory. The computations and theory support and enhance each other. A coherent approach was used which depends upon abstracting important mathematical concepts and computational methods from individual applications to a wide range of applications involving complex continua, including wave refractions, flows in elastic and plastic media, and complex fluid mixing. Adaptive computational methods were developed for flows with discontinuities and implemented on modern parallel computers.

14. SUBJECT TERMS

Front Tracking, Nonlinear Waves, Mathematical Concepts, Fluid Mixing, Wave Interactions

15. NUMBER OF PAGES

12

16. PRICE CODE

17. SECURITY CLASSIFICATION OF REPORT	18. SECURITY CLASSIFICATION OF THIS PAGE	19. SECURITY CLASSIFICATION OF ABSTRACT	20. LIMITATION OF ABSTRACT
UNCLASSIFIED	UNCLASSIFIED	UNCLASSIFIED	UL

ARO 26616.26-MA

FRONT TRACKING AND THE INTERACTION OF NONLINEAR WAVES

FINAL REPORT

May 13, 1992

U. S. ARMY RESEARCH OFFICE

Contract/Grant Number DAAL03-89-K-0017

Principal Investigators: James Glimm and John W. Grove

Department of Applied Mathematics
University at Stony Brook
Stony Brook, NY 11794-3600

Contents

1 Forward

Our research program has emphasized innovative computations and theory. The computations and theory support and enhance each other. We have a coherent approach which depends upon abstracting important mathematical concepts and computational methods from individual applications to a wide range of applications involving complex continua, including wave refractions, flows in elastic and plastic media, and complex fluid mixing. We have also developed adaptive computational methods for flows with discontinuities and implemented these methods on modern parallel computers.

2 List of Appendixes

There are no appendixes in this report.

3 Report of Research

3.1 Statement of Problem Studied

3.2 Summary of Most Important Work

3.2.1 Discontinuities and Adaptive Computation

The front tracking method [9], [20] is a computational method that incorporates explicit degrees of freedom to represent dynamical interfaces and wave interaction fronts. The method is highly developed in two space dimensions, and allows the resolution of complex, chaotic interfaces between two interpenetrating fluids [18]. It also allows for the refraction of shock waves by interfaces in a number of cases.

Interface methods (such as front tracking) are the only computational methods to duplicate the experimentally correct growth rate of the mixing zone for Rayleigh-Taylor unstable interfaces [16], [21]. Front tracking has provided the best and most extensive computations for this problem to date. In contrast, modern finite difference methods without interface methods have yielded values about 30% too low in comparison to experiment for the growth rate [36]. In spherical geometry, they display severe mesh orientation effects as well [1]. Front tracking computations were used in systematic studies of single and multi-mode Rayleigh-Taylor interactions, as shown for example in Figure 1, to establish the dynamics of elementary multiphase configurations [21] of interacting bubbles. The same computations are now being used to test turbulence models and multiphase flow models in the high Mach number compressible context [19].

Our main results are (a) parallelization, (b) three dimensional tracked computations (in progress), (c) complex wave interactions well resolved on a coarse grid and (d) the use of interface methods in tabular equations of state for multiphase materials.

A. Parallelization. The parallelization of the purely hyperbolic component of the two-dimensional front tracking code has been fully implemented on the INTEL iPSC/860 hypercube, enabling the parallel computation of gas dynamics problems. This parallelization was achieved by domain decomposition [13], [12], [11], [14]. The spatial domain is divided into a union of disjoint rectangular subdomains, with the accompanying division of the tracked physical discontinuity curves among the subdomains. An extended boundary region of n mesh blocks in each direction surrounds each subdomain providing overlap into neighboring subdomains. Typically n is an upper bound for the finite difference method's stencil radius, for example $n = 2$ for the Lax-Wendroff method. Thus, the boundary region for the i, j mesh block lies entirely in the eight mesh blocks surrounding it (neglecting the slight complication of physical boundaries). In Figure 1, we show a typical interface for a complex fluid mixing process, decomposed into 16 subdomains, with the overlapping boundaries displayed as well.

The tracking algorithm progresses iteratively as:

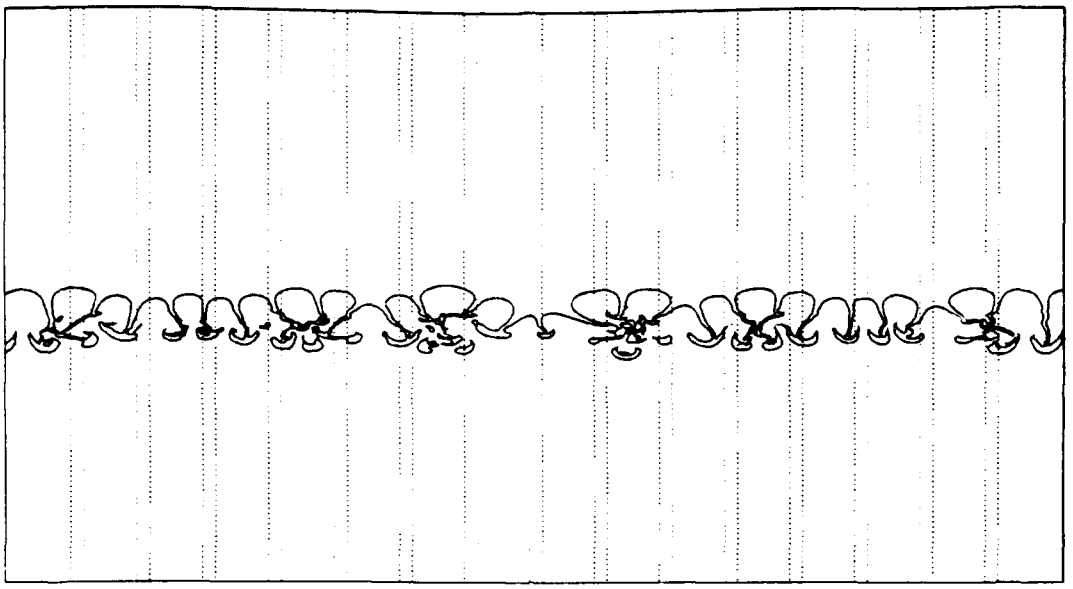

Figure 1: A typical interface at later time on a two-dimensional 320 × 300 mesh is decomposed into 16 sub-interfaces. The dotted vertical strips shown here are the overlapping border domains shared by neighboring processors.

1. Each subdomain updates those boundary regions of neighboring subdomains that lie inside its own area. (A subdomain never updates its own boundary region, which lies entirely within neighboring subdomains.)

2. The discontinuities are propagated and solution obtained for the next time step solely within each subdomain, using boundary data from its boundary region, which is stored on local memory.

This scatter–gather type of algorithm is most efficient if all subdomains are equally busy during step 2. This requires a sub–domain assignment algorithm which will produce subdomains, not of equal measure in spatial volume but of equal measure in propagation/solution update work. At present, a rather simple sub–domain assignment is in place. Current gas dynamics calculations have shown the parallelized code to be running at an efficiency of approximately 90%. The scientific power can be seen from the observation that the full parameter study [8] from which Figure 1 is extracted would have taken an estimated 17 years to complete on a Sun Microsystems SPARCstation1.

B. Three dimensional computations. Of critical physical interest is the ability to do computations in three spatial dimensions. We have begun this development for the front tracking code. Algorithms for triangulating surfaces in three dimensions and for re–gridding dynamical points of the surfaces have been implemented. A preliminary algorithm for generating volume filling grids which match moderately complicated surfaces was constructed but further work in this area is required. Additionally, data structures and code changes to handle arbitrary (spatial) dimensionality have been implemented into the front tracking code to support calculations in 1-, 2- and 3-dimensions.

C. Complex wave interactions. The analysis of the transitions from regular to irregular refractions of shock waves through material interfaces has resulted in an improved understanding of this process. The ideas developed here were applied to the passage of a shock wave through a bubble [27], yielding a substantial improvement in numerical resolution of the refractions. Figure 2 shows illustrates the production of an anomalous wave refraction during the shock–bubble interaction. As a result of this work, it was shown that the analysis of elementary waves given in [20] was incomplete due to an overly restrictive genericity

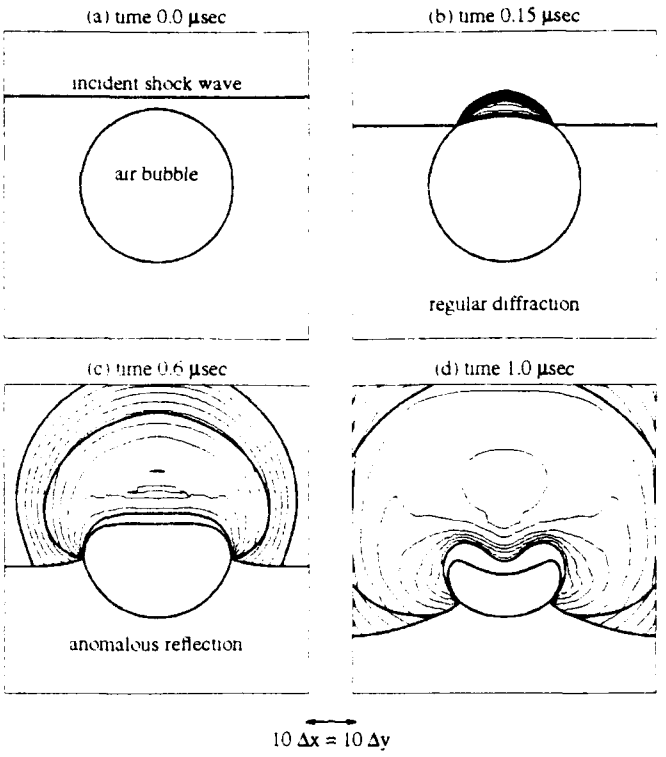

Figure 2: The collision of a shock wave in water with an air bubble. The fluids ahead of the shock are at normal conditions of 1 atm. pressure, with the density of water 1 g/cc and air 0.0012 g/cc. The pressure behind the incident shock is 10 Kbar with a shocked water density of 1.195 g/cc. The grid is 60×60. The contours in Figure 2.b and Figure 2.c are plotted on a scale of 0.001 - 10 Kbars, while the pressure range in Figure fg:anom.d is 0 - 8.5 Kbars. The tracked fronts are shown in a dark line superimposed on the pressure contours.

assumption, and that at least one additional elementary node, the total internal reflection, must be allowed. Subsequent work has applied these ideas to the Richtmyer-Meshkov problem of a shock accelerated fluid interface [19]. It was argued [26] that for the transition of a regular (self-similar) shock refraction into an irregular configuration, transitions can be classified into five basic cases depending on the shock impedance across the interface and on whether the reflected wave is a shock or rarefaction. This classification provides the background necessary to incorporate the complex configurations produced by irregular shock refractions into the front tracking method. Figure 3 illustrates one such complex interaction that occurs for a slow-fast interaction of a shock with a fluid interface. Here we see that after transition the original transmitted wave moves ahead of the incident shock, leading to a complex cascade of secondary wave interactions. Note that the detail of wave interaction resolved with front tracking in one or two grid blocks might take close to one hundred grid blocks for comparable resolution by other methods. The analysis and numerical implementation of the scattering behavior of irregular shock refractions is an essential component for full scale front tracking simulations of shock accelerated interfaces. The late time mixing behavior of the interface initially shown in Figure 3 is given in Figure 4. It should be noted that at this point the fluid interface is strongly affected by shock reflections from the nearby wall at the bottom of the computational domain.

D. Interface Methods for Tabular Equations of State. The front tracking software was used

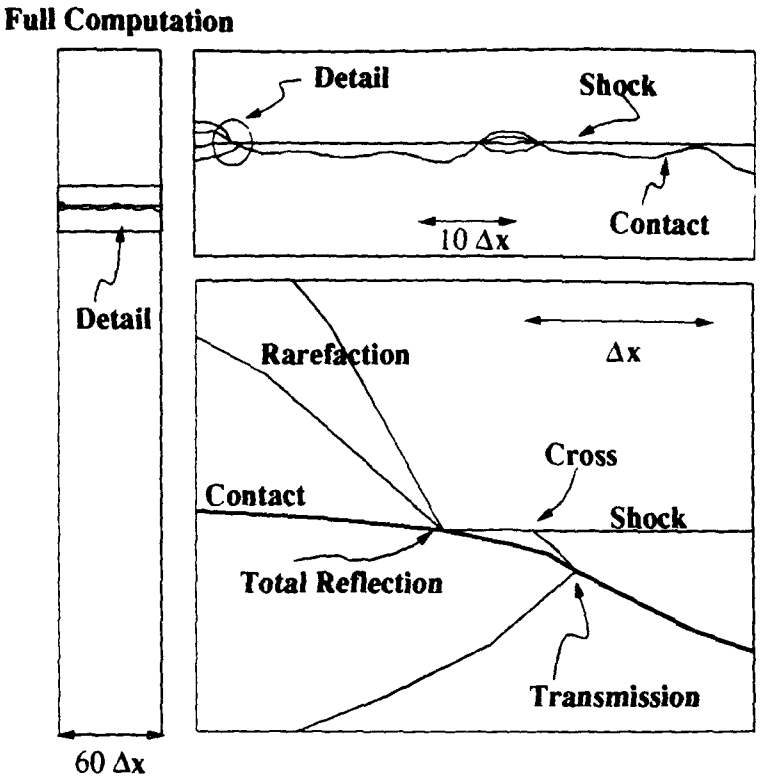

Figure 3: The passage of a shock wave through a random interface separating two gases of differing densities. The computation is shown together with two levels of graphical enlargement. At transition, the transmitted shock is moving faster than the incident shock leading to the production of a precursor wave. In the finest enlargement, one can see complex wave diffraction patterns resolved down to the level of a single mesh block, displaying a unique capability of front tracking. The long time behavior of this solution (Figure 4) exhibits interface instability similar to that of Figure 1.

as an interpolation scheme for piecewise smooth but discontinuous data. This method was applied to the representation of data in EOS tables with phase transitions [10]. Starting from original data given on a coarse grid, spline interpolation was used as an initialization, to give piecewise smooth data defined on a finer grid. Lower order but computationally more efficient linear-bilinear interpolation was used to interpolate the functions on the fine grid. This mapping of data from coarse to fine grid is computationally expensive, but is only performed once. For repeated evaluations, a significant improvement in the quality of the interpolated data was obtained in this way, see Figure 5. This interpolated, piecewise smooth data was then used to solve Riemann problems for gasses with a real equation of state. It was found that a real gas EOS Riemann problem could be solved in no more than about 3 to 8 times the time required for a γ - law gas. This efficiency depended on the use of precomputed and preinverted tables for the sound speed, the Riemann invariants and for thermodynamic variables expressed as a function of various combinations of independent variables. With the use of additional tables, a time at most 3 times the γ - law gas could have been achieved in all cases studied [35].

Figure 4: A detail showing the late time chaotic mixing resulting from the acceleration of a fluid interface by a shock wave. The figure shows the late time mixing zone for the simulation described in Figure 3. The detail is taken from the bottom of the computational cell and shows the shape of the fluid interface from Figure 3 500 microseconds after the shock collision.

3.2.2 Chaotic Flows

Our results provide a growing body of knowledge for the Rayleigh-Taylor mixing layer, with agreement among theory, experiment and direct simulation for nearly incompressible flows. We also found a surprising new phenomenon, discovered computationally, for compressible flows, in a substantially increased growth rate of the mixing layer, and a loss of universality which characterized the incompressible case.

The mixing process is characterized by a penetration height $h(t)$, which measures the distance of the most advanced bubble from the position of the unperturbed interface. This height obeys a scaling law $h = \alpha t^2$, in which the growth constant is found to be a universal constant $\alpha = .06$ in the incompressible experiments of Read and Youngs. We found agreement with this experimental growth rate in our nearly incompressible computations [21] and [22], but found surprising new phenomena for even moderately compressible fluids, namely, the mixing rate α may exceed twice its incompressible value. In addition, some loss of universality was observed through dependence of the growth rate on details of specification of the ensemble of initial conditions [8], [7]. The dependence of the growth rate α on dimensionless compressibility M^2 is shown in Figure 6.

In [23], [24], and [25] a statistical, chaotic theory of the Rayleigh-Taylor mixing layer is given in terms of a renormalization group fixed point model. The renormalization approach is used since the chaotic mixing layer involves dynamically changing length scales. The model is validated by comparing the predicted growth rate of the mixing layer with experiments and numerical computations [37]. The three main

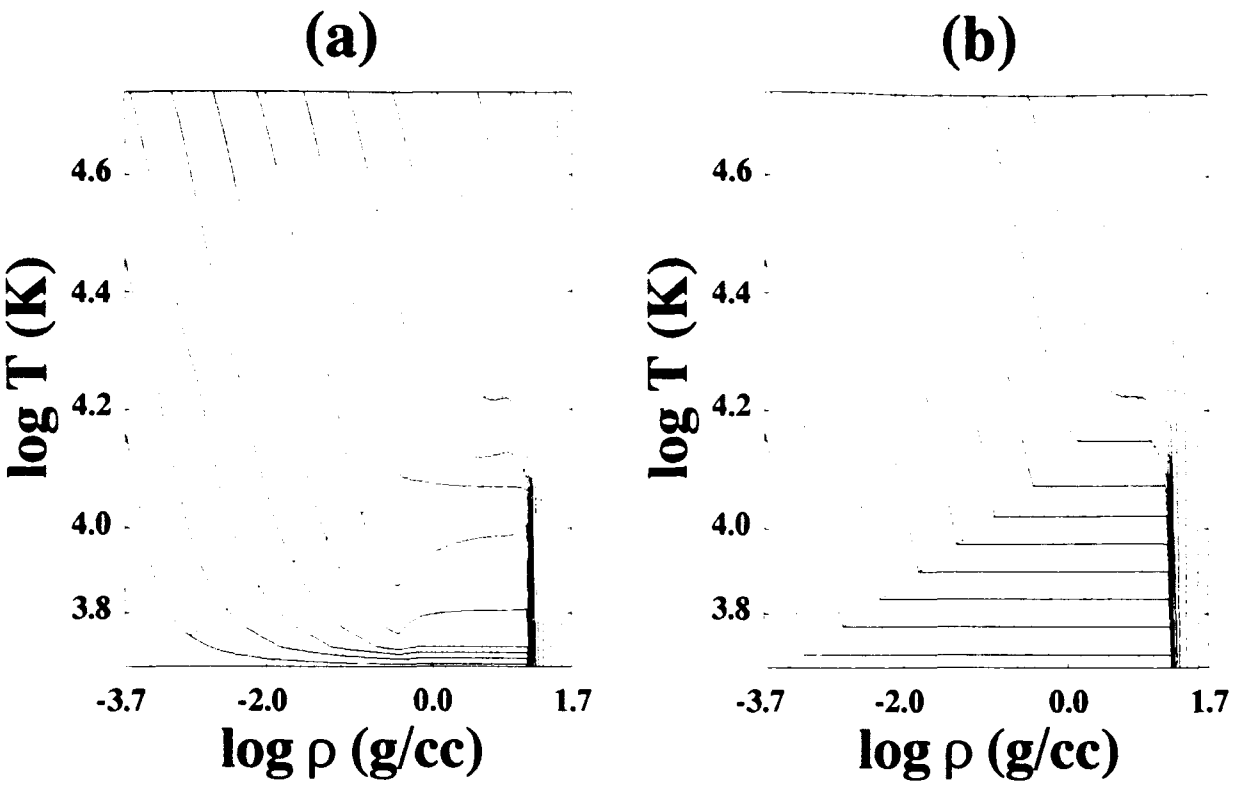

Figure 5: A comparison of isobars for tabulated equations of state. The plot on the left shows the computed isobars for a SESAME [31] equation of state near a phase boundary. Since the rational interpolator used in SESAME does not account for the discontinuous derivatives near the phase boundary, the resulting isobars are inaccurately represented in this region. The plot on the right shows the computed isobars obtained by the interface based interpolator which accurately represent the equation of state properties of the fluid near phase transition. Both plots are shown with the phase boundary curve superimposed as a dotted line over the isobars.

ingredients of this fixed point analysis are (a) a superposition hypothesis to specify the bubble – bubble interaction dynamics, (b) a theory of single bubble dynamics, (c) a statistical model to incorporate the above solutions to the one and two body problems for the bubble dynamics.

The superposition hypothesis was given in [21] and [22]. It describes the motion of the outer envelope in the Rayleigh-Taylor mixing layer as a superposition of individual bubble envelopes. The superposition theory explains the phenomenon that the velocity of a more advanced bubble in a multi-bubble system exceeds the velocity of a bubble of the same size in the single bubble system. This theory also explains the fact that a less advanced bubble in a multi-bubble system changes its direction of movement at the end of its period of interaction with a more advanced neighboring bubble. The superposition hypothesis has the virtue of containing no free parameter. The predictions of the superposition hypothesis are confirmed, to within the accuracy of the experiments, for the incompressible case by analysis of the experiments of Read. Comparison with numerical computations for compressible fluids shows agreement with the superposition hypothesis for small compressibility values, but reveals disagreement for larger values of compressibility, outside the range covered by experiments. An explanation for the disagreement and a possible basis for modification of the superposition hypothesis is given in terms of density stratification of the fluids. Disagreement is also noted in the cases where bubble splitting occurs, presumably due to omission of high

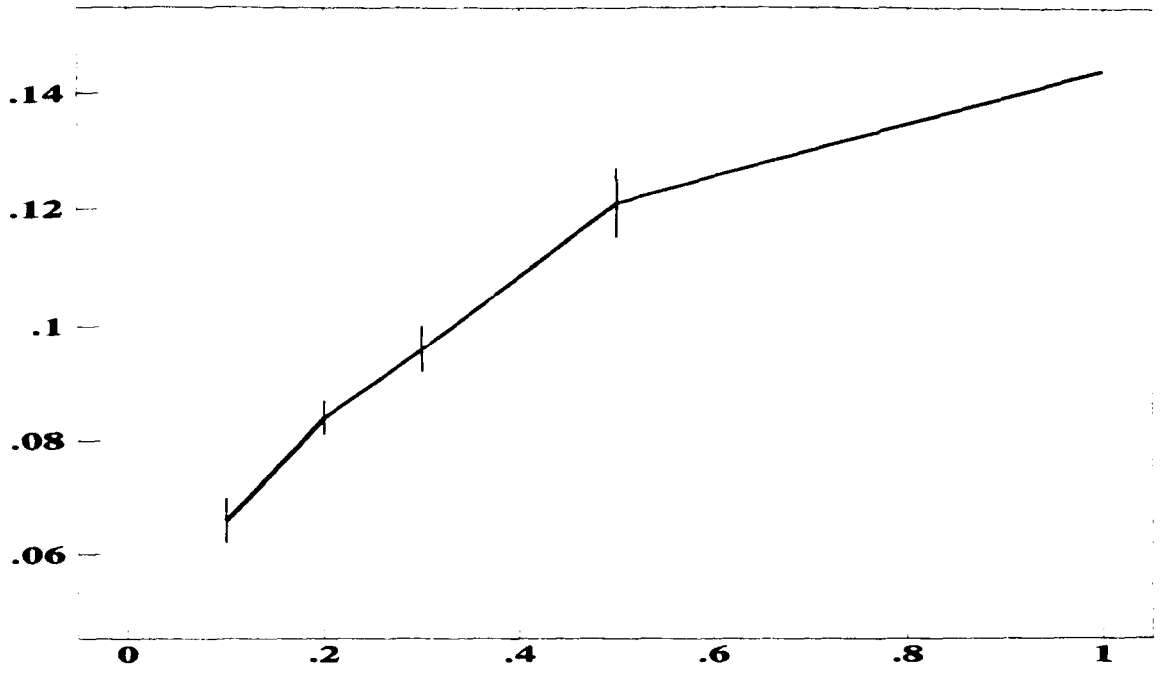

Figure 6: Plot of the growth rate constant vs. the compressibility. The vertical bars indicate the variance associated with the choice of random number seed.

frequency bubble splitting modes in the envelope description. Unexplained disagreement for computations at small Atwood number is also noted.

The superposition theory depends critically on a good description of the single (periodic) bubble dynamics. An extension of a previous theory for the growth of a single bubble with periodic boundary conditions, from a three parameter ODE to a four parameter ODE, was presented to remove an earlier ansatz which lacked physical basis. Two of the four parameters of the new theory are determined. The remaining two must be determined through explicit numerical calculations. Such a determination, over a limited range of the independent variables (Atwood number A and dimensionless compressibility M^2) was presented [22].

The statistical model on which the renormalization group fixed point is based describes an ensemble of bubbles of the same radius, whose heights are defined by a uniform probability measure restricted to a bounded interval. The statistical dynamics of flow with bubble merger is developed by treating pairwise interactions by drawing two adjacent bubbles randomly from the ensemble. The dynamics of each pairwise merger is given by the superposition hypothesis of [21], namely that, before merger, each bubble moves with a velocity given as the sum of a scaled single-bubble velocity, as treated in [22], and an envelope velocity. The bubble of higher height doubles in size and the lower bubble is removed from the statistical ensemble at the end of the merger. Differential equations are then obtained for the common radius, average height and variance of height of the ensemble of bubbles as a function of time. The variance of height is shown to have a natural interval. Its lower limit is a trivial fixed point corresponding to an (unstable) interface consisting of bubbles of identical height. Its upper endpoint is defined by instantaneous merger for bubble pairs of extreme separation. By studying the behavior of the rate of change of variance with time at these two endpoints, the existence of a non-trivial fixed point is shown. Figure 7 shows a numerical verification of this renormalization group fixed point for the Rayleigh-Taylor instability.

An extensive body of experiment and computation predicts a constant acceleration for the leading edge

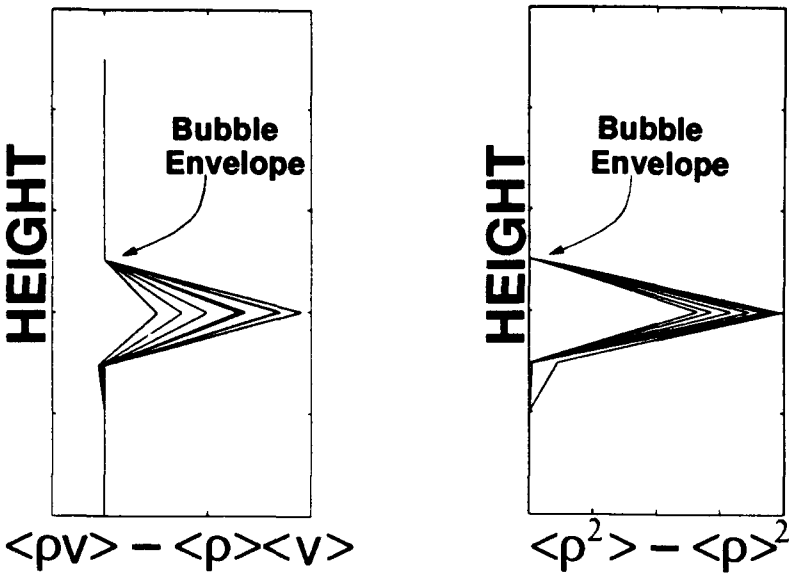

Figure 7: The numerical verification of a renormalization group fixed point for the bubble envelope of a Rayleigh-Taylor unstable interface. The graphs shown here represent the superposition of distinct time steps. Both axes are scaled by the renormalization group dynamics. The fixed point of the bubble envelope is shown in each graph. For the second correlation, on the right, the entire graph is approximately fixed in scaled variables.

of this mixing region, consistent with the conclusions of the fixed point predicted by this theory. The upper and lower limits placed on the value of the fixed point in this theory, are shown to yield upper and lower limits for this constant acceleration that are in full agreement with experiments and computations on incompressible and nearly incompressible systems. Further studies of the theory, including prediction of transient behavior, dependence on density ratio and compressibility, assumptions on uniform bubble radius, and extension to three dimensions remain to be carried out.

We are now studying the interior of the mixing zone itself, using computational data from well resolved direct simulation. Statistical analysis of fluctuating quantities reveals structure which is more complex than simple diffusion [8], [7]. In particular, steady acceleration (Rayleigh-Taylor unstable) induced mixing of a randomly perturbed interface shows non-monotone density contours and interior structure in second order correlations of fluctuating quantities. This is consistent with theories of turbulent boundary layers, which show at least three distinct regions within the mixing layer. The study of fluctuating quantities suggests renormalization group fixed point behavior near the edge of the mixing zone only and in the nearly incompressible case only [8], [7].

3.2.3 Nonlinear Waves and Nonlinear Materials

Striking new developments in the theory of nonlinear waves for conservation laws have given rise to a new picture for wave interactions in the large. Improved computational algorithms and modeling of physical phenomena are to be expected as the consequences of these results are explored. It is now widely recognized that nonlinear waves may contain two or more significant length scales. As a consequence the ratios of these length scales become important dimensionless parameters, controlling macroscopic wave speed and structure [29] for three phase flow, chemically reactive flow, elasticity and MHD waves [3].

Plohr, Marchesin et. al. [28] have produced a very important unifying framework for the fundamental

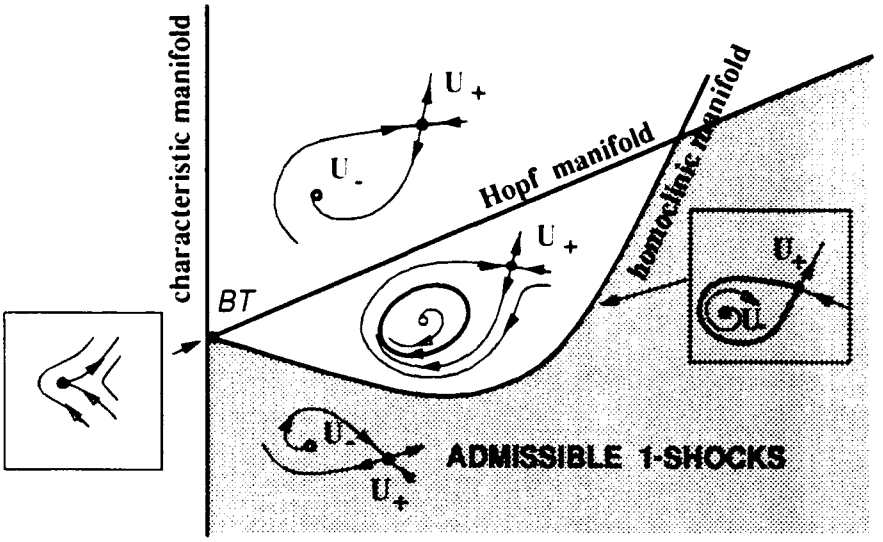

Figure 8: Shown here is a two dimensional slice of the wave manifold $\mathcal{W}$ for a representative 2×2 system of conservation laws with an elliptic region. The figure shows the influence of Hopf bifurcation on the admissibilty of shock waves, when the viscous admissibility criterion is taken into account. The connecting orbit, oriented from U_- to U_+, represents a traveling wave between these two states, i.e. a viscous-admissible shock wave. The figure shows a "bubble" region in which the connection between U_- and U_+ is prevented by the occurence of a limit cycle, which starts at the Hopf manifold. The limit cycle ends in the homoclinic loop, beyond which the connection from U_- to U_+ is established. The five phase diagrams, with associated singular points U_- and U_+, show orbits in the three open regions to the right of the characteristic manifold, and at two transitional boundary points. Only the shocks in the shaded region are admissible.

waves occurring in general systems of n conservation laws. By using a local change of coordinates, the Rankine-Hugoniot relation is shown to take the form $\mathcal{R} \cdot \mathcal{F} = 0$. The solution set where $\mathcal{R} = 0$ is a trivial solution set representing constant states and rarefaction waves. By eliminating this trivial solution set, it is shown that the solution set $\mathcal{W}$, where $\mathcal{F} = 0$, is a smooth manifold of dimension $n + 1$ and is the closure of the set of shock points. $\mathcal{W}$ is termed the fundamental wave manifold. Significantly, both rarefaction and shock waves are represented within $\mathcal{W}$, in accordance with the heuristic idea that shocks of infinitesimal strength are infinitesimal rarefaction fans. The rarefaction points form an n dimensional submanifold $\mathcal{C}$ of $\mathcal{W}$, the characteristic manifold, which may have singularities at points corresponding to coincident wave speeds. The familiar rarefaction curves in state space for the system of conservation laws are projections of a single family of curves in $\mathcal{C}$ which form a one dimensional foliation of $\mathcal{C}$. Correspondingly, the manifold $\mathcal{W}$ is foliated by two families of curves, called shock curves since they project onto the classical shock curves in state space. The work shows how this wave manifold framework can shed light on two fundamental problems in the theory of conservation laws. The first is the physical admissibility of shock waves determined by properties of dynamical systems parameterized by the points of $\mathcal{W}$. The second problem is the bifurcation of wave curves, which correspond to loss of transversality between rarefaction, shock, and composite foliations, and to the boundary of the region of admissible waves.

The wave manifold, $\mathcal{W}$, contains many nonadmissible shock waves. The most fundamental notion of admissibility presently known is the viscous profile criterion, which states the shock wave must be the limit,

as the viscosity tends to zero, of traveling waves for an associated viscous conservation law. This viscous conservation law gives rise to a dynamical system with critical points corresponding to the states on the left and right of the shock wave. In [6], some of the mathematical issues which will be associated with loss of admissibility are studied. Of particular interest is the demonstration that Hopf bifurcation can be the mechanism which leads to loss of admissibility. Similarly, homoclinic orbits are associated with a loss of admissibility. In Figure 8 we see that the connecting orbit bifurcates when crossing the Hopf bifurcation locus, so that one end is connected to the limit cycle emerging from the Hopf bifurcation. The connection between the end states of the shock wave is thus broken, implying the nonadmissibility of this shock wave.

The transitional waves are the most curious of the novel shock waves discovered in the recent renewal of interest in Riemann problems. These waves have dynamical system orbits which connect saddle points to saddle points, and thus they appear to be inherently unstable. However, they have been essential to obtain a satisfactory existence and uniqueness theory for solutions of Riemann problems. Stability analysis has been used in the search for a more satisfactory basis for accepting these waves as physically meaningful. In [38] nonlinear stability was studied, and on a numerical level, established for these shock waves.

Modeling of phase transitions was shown to depend on an additional degree of freedom (the order parameter), enlarging the system to give internal structure [17]. T.-P. Liu in his earlier work on nonequilibrium thermodynamics [30] also considered a larger system as a regularization of a smaller one. Related studies of the phase field model of phase boundaries [4], [5] follow this point of view. The relation between kinks and the loss of convexity in the equation of state and multiple or split waves in Riemann problems was developed in a systematic fashion in [32].

A fully conservative Eulerian formulation of the elasticity equations [33], [34] has recently been obtained. This formulation promises to be of considerable importance. In cases of large deformation, Eulerian computations are necessary to avoid the severe mesh distortion of Lagrangian grids. A thermodynamically consistent form of the elasticity constituitive laws derived from a free energy with a small deviatoric strain was given [33], [34]. This formulation allows arbitrary fluid behavior in the pressure and thermal modes, and depends on a single shear modulus to describe shear strength. It was shown that this formulation is the lowest order approximation to a general free energy in the case of a small deviatoric strain. An elasticity Riemann solver was constructed for this case. Computations have shown the distinct advantage of the fully conservative approach [2], [15].

In our study of nonlinear materials, a new and fully conservative formulation of plasticity was also formulated [34]. Based on the importance of the conservation formulation for computations in gas dynamics, we expect that this discovery could be of very fundamental character.

3.3 Publications and Technical Reports

1. J. Glimm, *Nonuniqueness of Solutions for Riemann Problems*, in "Nonlinear Hyperbolic Equations - Theory, Computation Methods, and Applications", eds. J. Ballmann & R. Jeltsch, Notes on Numerical Fluid Mechanics, **24**, pp. 169–178 (1989).

2. J. Glimm, "The Continuous Structure of Discontinuities," in *Lecture Notes in Physics*, vol. 344, *PDEs and Continuum Models of Phase Transitions*, ed. M. Rascle, D. Serre, and M. Slemrod, pp. 177-186, Springer–Verlag, 1989.

3. John W. Grove, "Anomalous Waves in Shock Wave - Fluid Interface Collisions," *Contemporary Mathematics*, vol. 100, *Current Progress in Hyperbolic Systems: Riemann Problems and Computations*, ed. W. B. Lindquist, (1989).

4. James Glimm, *Scientific Computing: von Neumann's Vision, Today's Realities and the Promise of the Future*, in "The Legacy of John von Neumann", eds. J. Glimm & J. Impagliazzo, Amer. Math. Soc., Providence, To Appear, (1989).

5. John Grove, *The Interaction of Shock Waves with Fluid Interfaces*, Adv. Appl. Math. **10**, pp. 201–227 (1989).

6. J. W. Grove, R. Menikoff, & Q. Zhang, "Unstable Interfaces and Anomalous Waves in Compressible Fluids," *Proceedings of the Seventh Army Conference on Applied Mathematics and Computing*, (1990).

7. John W. Grove & Ralph Menikoff, "Anomalous Reflection of a Shock Wave at a Fluid Interface," J. Fluid. Mech. vol. **219**, pp. 313-336, 1990.

8. Yuefan Deng & James Glimm, "Parallel Computations Using Interface Methods for Fluid Dynamics in Three Dimensions", *Proceedings of the Parallel CFD 90*, MIT Press (1990).

9. Yuefan Deng & James Glimm, "Fluid Dynamics Using Interface Methods on Parallel Processors", in *Proceedings of the IMACS First International Conference on Computational Physics*, North–Holland (1990).

10. J. Glimm, "A Review of Interface Methods for Fluid Computations", in *Computational Methods for Subsurface Hydrology*, eds. G. Gambolati, A. Rinaldo, C.A. Brebbia, G.F. Pinder, Springer-Verlag, New York, pp. 421–432, (1990).

11. J. Glimm, X. L. Li, R. Menikoff, D.H. Sharp, and Q. Zhang, "A Numerical Study of Bubble Interactions in Rayleigh-Taylor Instability for Compressible Fluids", Phys. Fluids A **2**(11), pp. 2046–2054, (Nov. 1990).

12. John W. Grove & Ralph Menikoff, "Anomalous Reflection of a Shock Wave at a Fluid Interface," in *IMA Volumes in Mathematics and its Applications*, eds. J. Glimm and A. Majda Springer–Verlag, (1990).

13. James G. Glimm & David H. Sharp, *Chaotic Mixing as a Renormalization Group Fixed Point*, *Physical Review Letters*, vol. 64, pp. 2137–2139, (1990).

14. J. Glimm, "Nonlinear and Stochastic Phenomena: The Grand Challenge for Partial Differential Equations," SIAM Review, vol. 33, no. 4, pp. 626–643, December 1991.

15. J. Glimm, J.W. Grove, Y. Chen, and X.L. Li, "Chaotic Mixing at Unstable Interfaces," Proceedings of Third International Workshop on The Physics of Compressible Turbulent Mixing at Royaumont France, (1991).

16. J. Glimm, Q. Zhang and D.H. Sharp, "The Renormalization Group Dynamics of Chaotic Mixing of Unstable Interfaces," Phys. Fluids A **3** (5), (1991).

17. J. Glimm and Q. Zhang, "A Quantitative Theory of Fluid Chaos," in *Viscous Profiles and Numerical Methods for Shock Waves*, ed. M. Shearer SIAM, Philadelphia, pp. 49–65 (1991).

18. John W. Grove, "Irregular Shock Refractions at a Fluid Interface," Proc. APS 1991 Topical Conf. on Shock Compression of Condensed Matter., (To Appear 1992).

19. J. Glimm, "Stochastic Partial Differential Equations and the Chaotic Mixing of Fluids," Proceedings of the 18th Brazilian Mathematics Collquium, Rio de Janeiro, Brazil, (To Appear 1992).

20. John W. Grove, "A Survey of the Analysis of Irregular Shock Refractions and its Application to Front Tracking Methods," Proc. of the Second Workshop on Hyperbolic Waves, Rio de Janeiro, Brazil, (To Appear 1992).

21. Q. Zhang and J. Glimm, "Inertial Scaling of Laminar Shear Flow as a Model of Turbulent Transport," Commun. Math. Phys., (To Appear 1992).

22. E. L. Isaacson, D. Marchesin, C. F. Palmeira, B. J. Plohr, "A Global Formalism for Nonlinear Waves in Conservation Laws," Commun. Math. Phys., (To Appear 1992).

23. Y. Deng, J. Glimm, D. H. Sharp, "Perspectives on Parallel Computing", Daedalus, pp. 31-52 (1992).

24. Y. Chen, Y. Deng, J. Glimm, G. Li, "A Renormalization Group Scaling Analysis for Compressible Two-Phase Flow", SUNYSB preprint, (1992).

3.4 Participating Scientific Personnel

Senior Personnel

1. James Glimm
2. John W. Grove
3. Yuefan Deng
4. Bradley Plohr

Students

1. S. Canic, Ph.D. Awarded June 1992
2. A. Chang
3. C. Soell
4. M. Stein
5. S. Tael
6. H. Wong
7. S. Mody
8. Q. Li
9. K. Nakayama,
10. R. Stingley
11. Y. Zhuge

4 Report of Inventions

There were no inventions produced during the tenure of this grant.